

1 **Delayed induction of type I and III interferons mediates nasal epithelial cell permissiveness to**
2 **SARS-CoV-2**

3 Catherine F Hatton^{1a}, Rachel A Botting^{2a}, Maria Emilia Dueñas^{2a}, Iram J Haq^{1,3a}, Bernard Verdon^{2a},
4 Benjamin J Thompson¹, Jarmila Stremenova Spegarova¹, Florian Gothe^{1,4}, Emily Stephenson², Aaron I
5 Gardner¹, Sandra Murphy², Jonathan Scott¹, James P Garnett¹, Sean Carrie⁵, Jason Powell¹, C M Anjam
6 Khan², Lei Huang¹, Rafiqul Hussain⁶, Jonathan Coxhead⁶, Tracey Davey⁷, A John Simpson¹, Muzlifah
7 Haniffa^{2,8,9,10}, Sophie Hambleton^{1,11}, Malcolm Brodrie^{1,3b}, Chris Ward^{1b}, Matthias Trost^{2b}, Gary
8 Reynolds^{2b}, Christopher J A Duncan^{1,12 b*}

9

10 **Supplementary Materials**

11

12 **Contents**

13 Supplementary Figures S1-10

14 Supplementary Tables S1-6

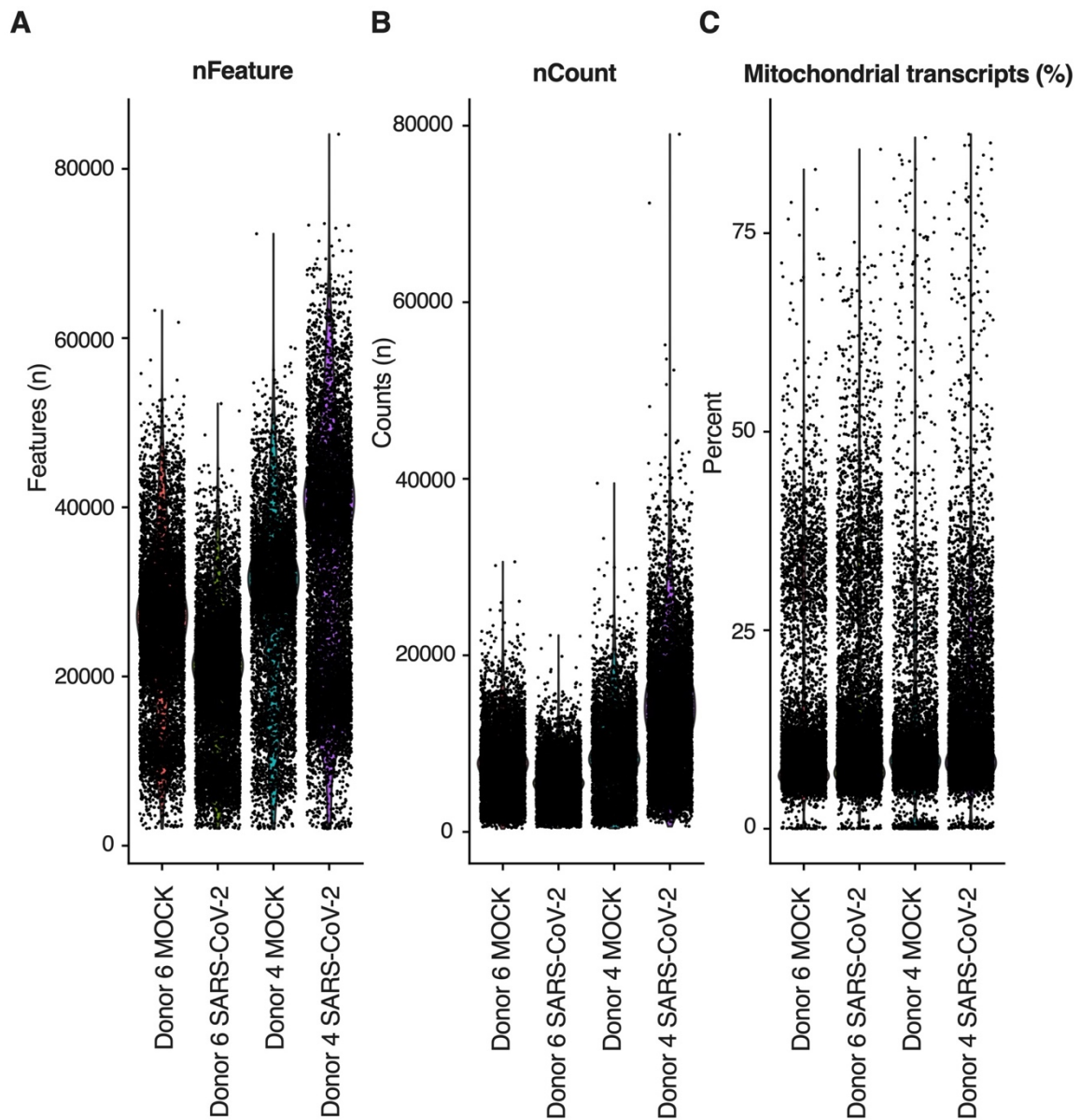
15 Supplementary Methods

16 Note supplementary datasets S1-5 (csv files) are not included in this file

17

18

19



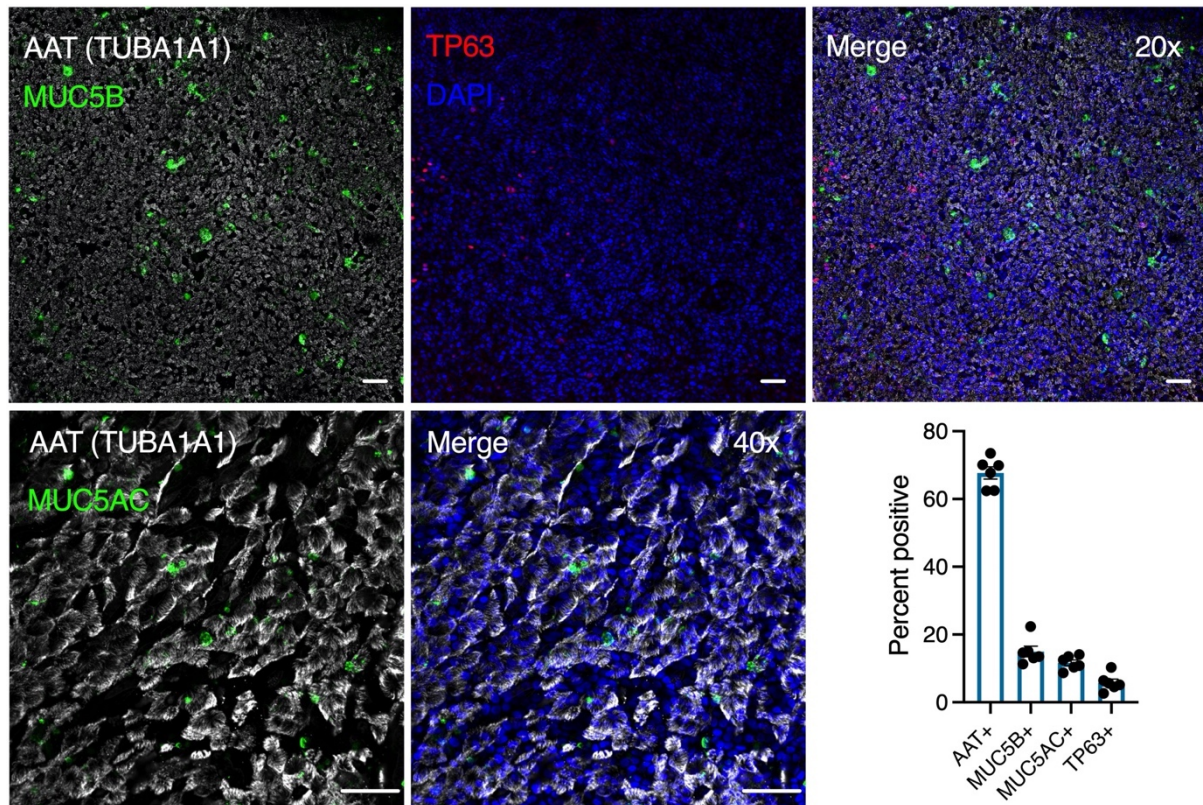
21

22 **Figure S1.** Single cell RNA sequencing quality control plots. Violin plots, split by sample, showing (A)

23 the total number of genes detected in each cell (B) the total number of counts detected in each cell

24 and (C) the proportion (as a percentage) of mitochondrial transcripts in each cell. For individual QC

25 metrics see also Table S1.



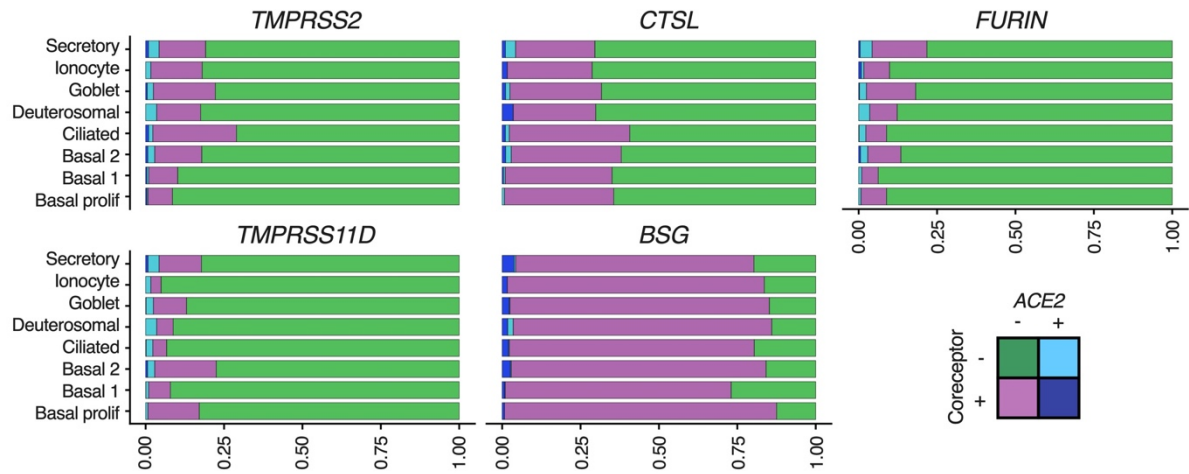
26

27 **Figure S2.** Immunofluorescence analysis of ciliated (AAT+), secretory (MUC5B+), goblet (MUC5AC+) and basal (TP63+) cells in nasal ALI cultures. Representative images from n=6 donors, scale bar = 20
 28 mm (top panel 20x magnification, bottom panel 40x magnification as indicated). Frequency of cell
 29 type as a proportion of cells counted is displayed in the bar plot. MUC5B and MUC5AC co-staining
 30 demonstrated no overlap in immunoreactivity (data not shown).
 31

32

33

34



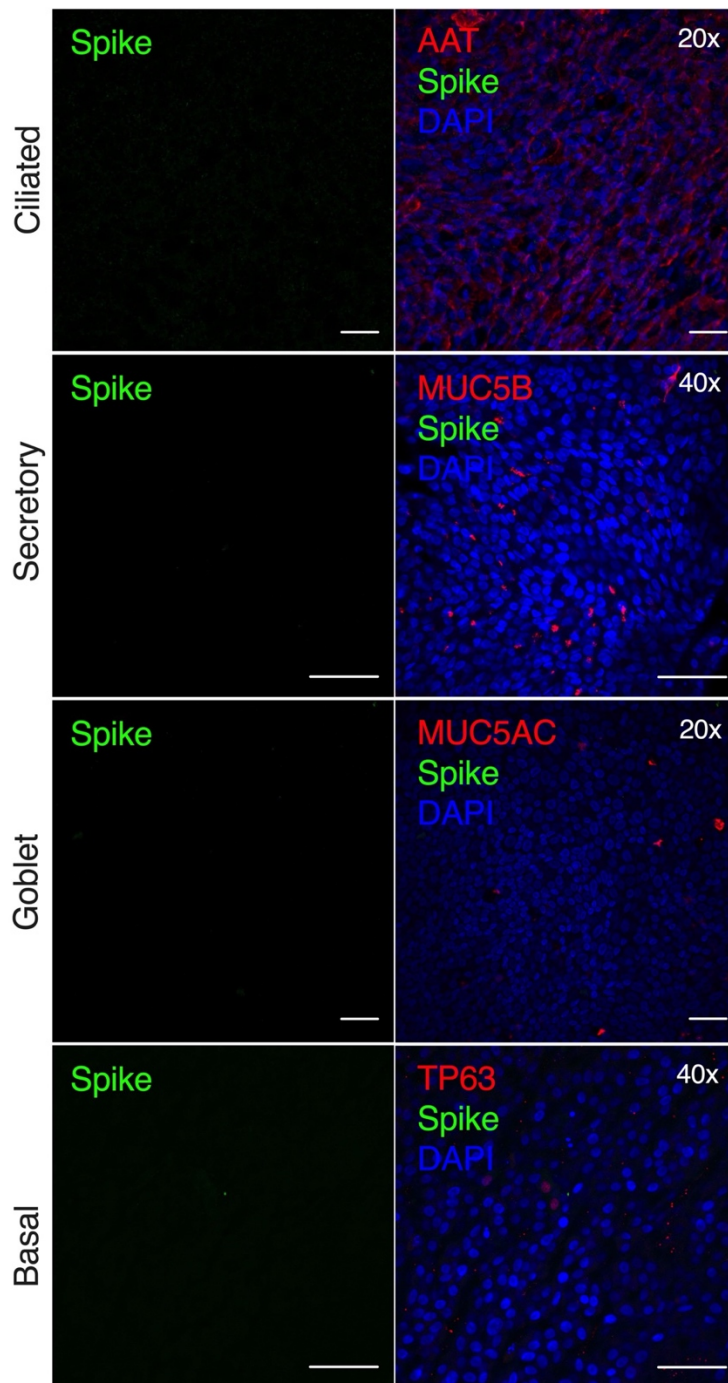
35

36 **Figure S3.** Single-cell RNA-seq analysis of entry receptor expression by cell type. Bars represent the
 37 proportion of cells expressing each combination of *ACE2* and other transcript, coloured according to
 38 the key. Dark blue represents the proportion of cells of each type expressing both *ACE2* and the
 39 relevant additional transcript. Data from analysis of 28,346 cells from n=2 donors.

40

41

42

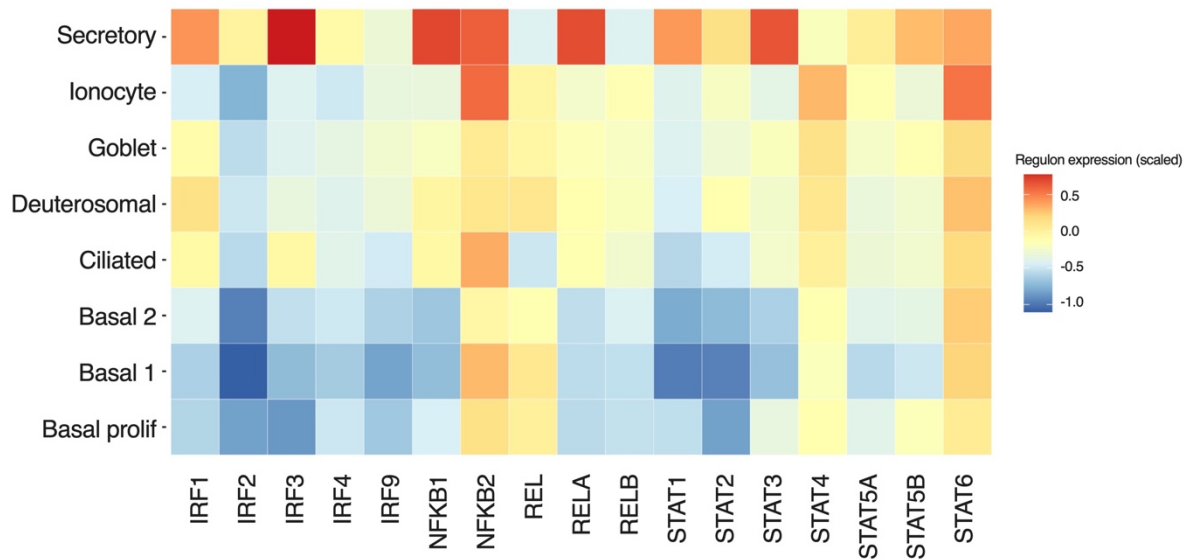


43

44 **Figure S4.** Immunofluorescence analysis of S protein immunoreactivity in mock infected nasal ALI
 45 cultures. Displayed are mock infected ciliated (AAT+), secretory (MUC5B+), goblet (MUC5AC+) and
 46 basal (TP63+) cells stained for S protein. Representative images from n=5 donors, scale bar = 20 mm
 47 (images at 20x or 40x magnification as indicated).

48

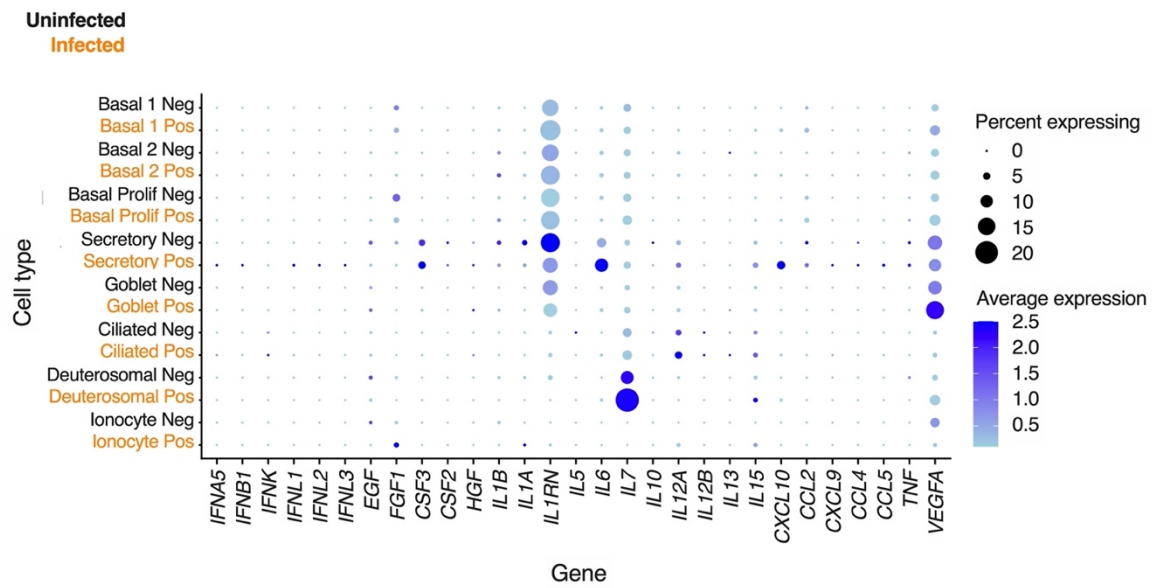
49



50

51 **Figure S5.** DoRoThea/VIPER analysis of regulon activity in infected cells. Median regulon activity per
 52 cluster in infected cells, corrected for activity in uninfected cells by subtraction then Z-normalised by
 53 TF (i.e. values > 0 imply TF more active in infected cells). Data from analysis of 28,346 cells total to
 54 estimate regulon activity of which 8,861 infected, from n=2 donors at 24 hpi.

55



56

57 **Figure S6.** Interferon, chemokine and cytokine induction in response to SARS-CoV-2. Dot plot showing

58 single-cell RNA-seq analysis of cytokine and chemokine transcript detection in n=2 donors at 24 hpi

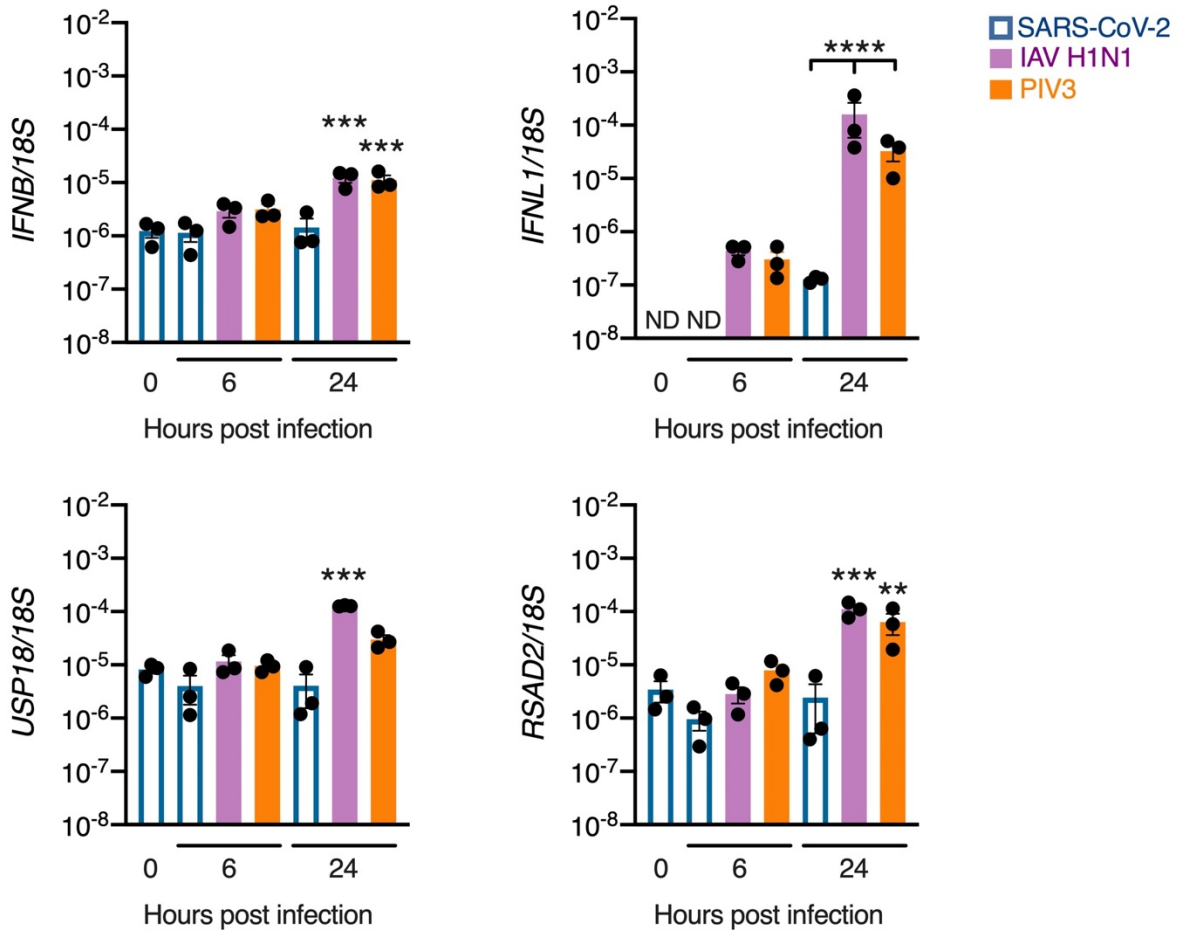
59 (size of dots represent proportion of cells expressing and colour represents mean expression).

60 Uninfected cells are labelled black (Neg) and infected cells orange (Pos) based on expression of SARS-

61 CoV-2 mRNA. Low-level induction of certain proinflammatory cytokines (*IL6*, *IL12A*, *IL15*), chemokines

62 (*CXCL9*, *CXCL10*) and *VEGFA* is demonstrated in SARS-CoV-2-infected nasal cells.

63



64

65 **Figure S7.** Delayed induction of IFNs and ISGs in response to SARS-CoV-2 compared to other viruses.

66 RT-PCR analysis of *IFNB*, *IFNL1*, *USP18* and *RSAD2* expression in nasal ALLI cultures mock infected (0h)

67 or exposed to SARS-CoV-2 (open bars), influenza A virus (IAV H1N1, purple bars) or parainfluenza 3

68 virus (PIV3, orange bars) for the times displayed, all at MOI 0.1 (n=3 donors, mean ± SEM; ANOVA with

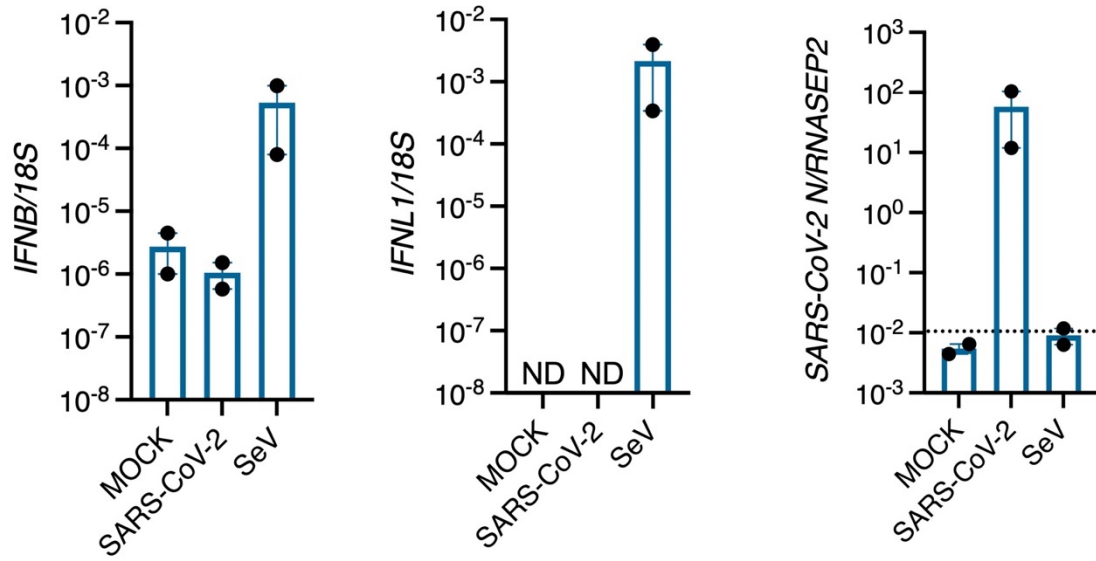
69 Dunnett's post-test correction compared to 0h, or Sidak's post-test correction [all viruses compared

70 at 24 hpi], ** P < 0.01 *** P < 0.01 **** P < 0.001). ND = not detected.

71

72

73



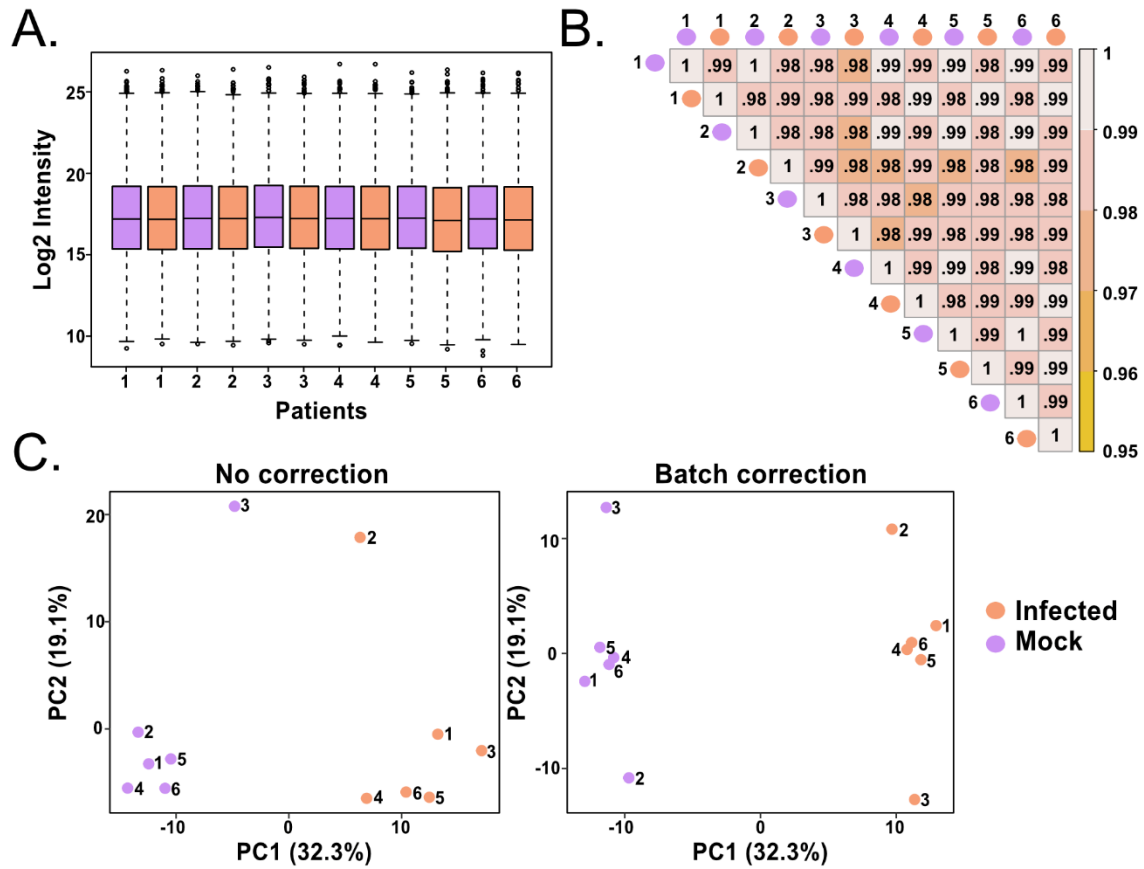
74

75 **Figure S8.** Robust nasal cell expression of *IFNB* and *IFNL1* in response to Sendai virus. RT-PCR analysis
 76 of *IFNB*, *IFNL1* and SARS-CoV-2 *N* gene expression in nasal ALI cultures exposed to SARS-CoV-2 (MOI
 77 2) or a DVG-rich stock of Sendai virus (SeV) for 6 h (n=2 donors, mean ± SEM). ND = not detected.

78

79

80



81

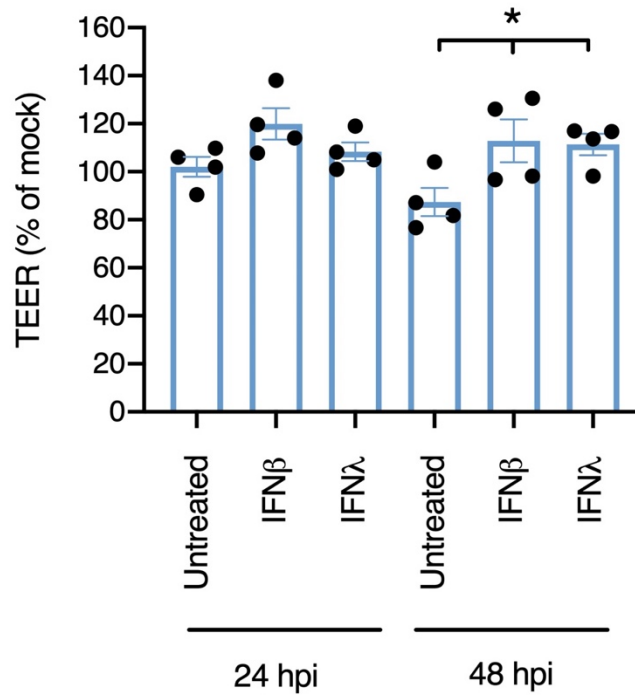
82 **Figure S9.** Quality control measures for the proteomics data set. (A) Boxplot of log₂ transformed
 83 samples shows equal loading. (B) Pearson correlation heatmap among the log₂ transformed samples
 84 shows high reproducibility between samples. (C) Principal component analysis plots with no correction
 85 (left) and after removing patient batch effects (right).

86

87

88

89



90

91 **Figure S10.** IFN treatment preserves barrier integrity in the face of SARS-CoV-2 infection. Trans-
 92 epithelial resistance measurement (expressed as % of mock infected controls) at 24 and 48 hpi (MOI
 93 0.01) were compared to cells pre-treated for 16h with IFNβ1 (1000 IU/mL) or IFNλ1 (100 ng/mL).
 94 Repeat experiments in n=4 donors, mean ± SEM; * P < 0.05, ANOVA with Sidak's post-test correction.

95

96

97

98

99

100 **Supplementary Tables**

Sample_id	Total number of reads	Mean reads per cell	Alignment rate (%)	Reads mapped to GRCh38 (5)	Reads mapped to SARS-CoV-2	Estimated number of cells
Donor4_Mock	184,897,338	14,329	91.3	91.3	0	12,904
Donor4_Infected	807,865,486	61,100	87.7	77.1	10.8	13,222
Donor6_Mock	232,499,890	17,121	90.4	90.4	0	13,580
Donor6_Infected	174,974,839	13,653	90	88.8	1.3	12,816

101

102 **Table S1.** Single cell RNA-seq post-alignment quality control metrics. Quality control output from

103 CellRanger following alignment.

104

105

GO_TERM	FDR Adjusted P value
Defence response to virus	4.5E-28
Type I interferon signalling pathway	2.3E-18
Response to virus	1.4E-13
Negative regulation of viral genome regulation	5.7E-11
Interferon gamma-mediated signalling pathway	5.8E-9
Innate immune response	7.6E-5
Intracellular transport of viral protein in host cell	6.9E-3
Negative regulation of type I interferon production	7.2E-3
Antigen processing and presentation via MHC class I	1.1E-2
Cellular response to interferon alpha	1.7E-2
Response to interferon alpha	2.0E-2

106

107 **Table S2.** Pathway analysis of proteomics data showing upregulated pathways. Displayed are

108 pathways with Benjamini-Hochberg false-discovery rate (FDR)-adjusted P value < 0.05 (5E-2).

109

110

GO_TERM	FDR Adjusted P value
TRIF-dependent toll-like receptor signalling pathway	1.5E-2
Regulation of transcription from RNA polymerase II promoter in response to hypoxia	1.5E-2
Endosomal transport	1.7E-2
MyD88-independent toll-like receptor signalling pathway	1.7E-2
Transcription-coupled nucleotide-excision repair	2.4E-2

111

112 **Table S3.** Gene Ontology (GO) Term analysis of proteomics data showing downregulated pathways.

113 Displayed are pathways with Benjamini-Hochberg false-discovery rate (FDR)-adjusted P value < 0.05

114 (5E-2).

115

116

117

118

Donor no.	Sex	Age (years)
1	Female	46
2	Female	38
3	Male	68
4	Male	78
5	Female	54
6	Male	41

119

120 **Table S4.** Nasal cell donors.

121

122

Gene	UPL probe	Forward sequence	Reverse sequence
<i>IFNB</i>	#25	CGACACTGTTTCGTGTTGTCA	GAAGCACAACAGGAGAGCAA
<i>IFNL1</i>	#75	GGGACCTGAGGCTTCTCC	CCAGGACCTTCAGCGTCA
<i>IL6</i>	#40	GATGAGTACAAAAGTCCTGATCCA	CTGCAGCCACTGGTTCTGT
<i>IL1B</i>	#78	TACCTGTCCTGCGTGTTGAA	TCTTTGGGTAATTTTTGGGATCT
<i>RSAD2</i>	#9	GAGGGTGAGAATTGTGGAGAAG	GCGCTCCAAGAATCTTTCAA
<i>USP18</i>	#44	CAACGTGCCCTTGTTTGTC	ATCAGGTTCCAGAGTTTGAGGT
<i>ISG15</i>	#23	GCGAACTCATCTTTGCCAGTA	CCAGCATCTTCACCGTCAG
<i>18S</i>	#81	CCGATTGGATGGTTTAGTGAG	AGTTCGACCGTCTTCTCAGC

123

124 **Table S5.** Primers/probes. UPL = Roche universal probe library.

125

Antibody	Host	Dilution	Source	Code
Spike	Rabbit	1:1000	Novus	nb100-56578
RSAD2	Rabbit	1:1000	CST	13996
ISG15	Rabbit	1:1000	CST	2743
USP18	Mouse	1:2000	SCB	sc-1668
ACE2	Rabbit	1:1000	Abcam	ab15348
ACE2	Goat	1:200	R&D	AF933
TMPRSS2	Rabbit	1:1000	Abcam	ab92323
MxA	Rabbit	1:1000	SCB	sc-50509
GAPDH	Rabbit	1:10,000	CST	5174
MUC5B	Rabbit	1:1000	Sigma	HPA008246
MUC5AC	Rabbit	1:1000	Sigma	HPA040615
TP63	Mouse	1:2000	Abcam	ab735
Acetylated-alpha tubulin	Mouse	1:1000	Abcam	ab24610
Anti-rabbit HRP- conjugated	Goat	Primary-dependent	CST	7074
Anti-mouse HRP-conjugated	Horse	Primary-dependent	CST	7076
AF488 conjugated anti-mouse	Goat	1:2000	TFS	A-11001
AF488 conjugated anti-rabbit	Goat	1:2000	TFS	A-11008
AF594 conjugated anti-mouse	Goat	1:2000	TFS	A-11005
AF594 conjugated anti-rabbit	Goat	1:2000	TFS	A-11012

126

127 **Table S6.** Antibodies. CST = Cell Signalling; SCB = Santa Cruz Biotechnology; R&D = R&D biosystems;

128 TFS = ThermoFisher Scientific. HRP = horseradish peroxidase.

129

130

131

132 **Supplementary Methods**

133

134 **Proteome sample preparation**

135 Cells were washed three times with cold PBS before addition of solubilisation buffer (5% (w/v) SDS, 50
136 mM TEAB) to the apical compartment for 10 min at room temperature (RT). Samples were heated at
137 75°C for 45 min, before freezing and stored at -80°C. Protein concentration was determined by EZQ®
138 protein quantification assay. A total of 30 µg protein was reduced by incubation with 5 mM tris(2-
139 carboxyethyl)phosphine for 15 min at 37°C, and subsequently alkylated with 20 mM iodoacetamide
140 for 30 min at RT in the dark. Protein digestion was performed using the suspension trapping (S-Trap™)
141 sample preparation method according to the manufacturer's guidelines (ProtiFi, USA). Briefly, 2.5 µL
142 of 12% phosphoric acid was added to each sample, followed by the addition of 165 µL S-Trap binding
143 buffer (100 mM TEAB in 90% methanol, pH 7.1). Samples were added to S-Trap Micro spin columns
144 followed by centrifugation (4,000 g, 2 min). Each S-Trap Mini-spin column was washed with 150 µL S-
145 trap binding buffer by centrifugation (4,000 g, 1 min). This process was repeated for a total of 4
146 washes. 25 µL of 50 mM TEAB, pH 8.0 containing trypsin (1:20 ratio of trypsin to protein) was added
147 to each sample, followed by proteolytic digestion for 3 hours at 47°C without shaking. Peptides were
148 eluted with 50 mM TEAB pH 8.0 and centrifugation (4,000 g, 2 min). Elution steps were repeated twice
149 more, using 0.2% formic acid and 0.2% formic acid in 50% acetonitrile, respectively. The three eluates
150 from each sample were combined and dried using a speed-vac before storage at -80°C.

151

152 **TMT-16 plex labelling**

153 Each 30 µg protein digest was resuspended in 25 µL 100 mM HEPES, pH 8.5. TMT-16 plex labelling
154 (TMT lot number: UI292951) was carried out as per the manufacturer's instructions. Samples were
155 assigned to a TMT tag. 10 µL of the corresponding TMT tag was added per sample and incubated for
156 1 hour at RT. An aliquot corresponding to 1 µg was taken from each sample and pooled together for
157 ratio and labelling efficiency checks, prior to making the full pooled sample. The test pool was

158 quenched with 0.69 μL of 5% hydroxylamine, incubated for 15 min at room temperature, and dried
159 using a speed-vac. The sample was cleaned using a C18 spin column as per the manufacturer's
160 guidelines (Thermo Scientific), and subsequently dried using a speed-vac. Peptides (dissolved in 5%
161 formic acid) from the pooled sample were analysed for labelling efficiency and ratio check. For the
162 ratio check, each sample (corresponding to a single TMT channel) was normalised to the average
163 summed intensity of all samples within its pool. Each sample was quenched with 2.5 μL 5%
164 hydroxylamine and incubated for 15 min. Subsequently, samples were pooled together based on the
165 scaling factors, which were calculated using the test pool. Samples were dried using a speed-vac,
166 cleaned using MacroSpin columns as per the manufacturer's guidelines (Harvard Apparatus, USA), and
167 dried down again using a speed-vac prior to offline high-performance liquid chromatography (HPLC)
168 fractionation.

169

170 **Offline HPLC Fractionation**

171 Peptides were resuspended in 80 μL ammonium formate, pH 8.0. Peptides were fractionated on a
172 Basic Reverse Phase column (Gemini C18, 3 μm particle size, 110A pore, 3 mm internal diameter, 250
173 mm length, Phenomenex #00G-4439-Y0) on a Dionex Ultimate 3000 off-line LC system. All solvents
174 used were HPLC grade (Rathburn Chemicals, UK). 40 μL of peptide sample were loaded onto the
175 column for 1 min at 250 $\mu\text{L}/\text{min}$ using 99% Buffer A (20 mM ammonium formate, pH 8.0) and eluted
176 for 40 min on a linear gradient from 1 to 90% Buffer B (100% acetonitrile (ACN)). Peptide elution was
177 monitored by UV detection at 214 nm. Fractions were collected every minute from 2 to 38 minutes
178 for a total of 36 fractions. Fractions were pooled using non-consecutive concatenation to obtain 18
179 pooled fractions (e.g. pooled fraction 1: fraction 1 + 19). Each fraction was acidified to a final
180 concentration of 1% TFA and dried using a speed-vac.

181

182 **Mass spectrometry**

183 Peptides were dissolved in 5% formic acid, and each sample was independently analysed on an
184 Orbitrap Fusion Lumos Tribrid mass spectrometer (Thermo Fisher Scientific), connected to an UltiMate
185 3000 RSLCnano System (Thermo Fisher Scientific). Peptides (~2 µg per fraction) were injected on an
186 Acclaim PepMap 100 C18 LC trap column (100 µm ID × 20 mm, 3 µm, 100 Å) followed by separation
187 on an EASY-Spray nanoLC C18 column (75 ID µm × 750 mm, 2 µm, 100 Å) at a flow rate of 200 nL/min.
188 Solvent A was 0.1% formic acid in H₂O and solvent B was 80% ACN containing 0.1% formic acid. The
189 gradient used for analysis of proteome samples was as follows: solvent B was maintained at 3% for
190 5 min, followed by an increase of solvent B from 3% to 35% in 120 min, 35% to 90% B in 0.5 min,
191 maintained at 90% B for 4 min, followed by a decrease to 3% in 0.5 min and equilibration at 3% for
192 20 min. Mass spectrometric identification and quantification was performed on an Orbitrap Fusion
193 Tribrid mass spectrometer (Thermo-Fisher Scientific) operated in data-dependent, positive ion mode.
194 Full scan spectra were acquired in a range from 375 m/z to 1500 m/z, at a resolution of 120,000, with
195 a standard automated gain control (AGC) (Tune 3.3) and a maximum injection time of 50 ms. Precursor
196 ions were isolated with a quadrupole mass filter width of 0.7 m/z and CID fragmentation was
197 performed in one-step collision energy of 30% and 0.25 activation Q. Detection of MS/MS fragments
198 was acquired in the linear ion trap in a rapid mode using a Top 3s method, with a standard AGC target
199 and a maximum injection time of 50 ms. The dynamic exclusion of previously acquired precursor was
200 enabled for 60 s with a tolerance of +/-10 ppm. Quantitative analysis of TMT-tagged peptides was
201 performed using FTMS3 acquisition in the Orbitrap mass analyser operated at 60,000 resolution, with
202 a standard AGC target and maximum injection time of 118 ms. HCD fragmentation on MS/MS
203 fragments was performed in one-step collision energy of 55% to ensure maximal TMT reporter ion
204 yield and synchronous-precursor-selection (SPS) was enabled to include 10 MS/MS fragment ions in
205 the FTMS3 scan.

206

207 **Mass spectrometry data analysis**

208 All spectra were analysed using MaxQuant 1.6.10.43 and searched against SwissProt *Homo*
209 *sapiens* (with 42423 sequences) and Trembl SARS-CoV-2 (with 107 sequences) FASTA files. Peak list
210 generation was performed within MaxQuant and searches were performed using default parameters
211 and the built-in Andromeda search engine. Reporter ion MS3 was used for quantification and the
212 additional parameter of quantitation labels with 16 plex TMT on N-terminus or lysine was included.
213 The enzyme specificity was set to consider fully tryptic peptides, and two missed cleavages were
214 allowed. Oxidation of methionine and N-terminal acetylation were allowed as variable modifications.
215 Carbamidomethylation of cysteine was allowed as a fixed modification. A protein and peptide false
216 discovery rate (FDR) of less than 1% was employed in MaxQuant. Reporter ion intensities were used
217 for data analysis. Briefly, the data were filtered to remove proteins that matched to a contaminant or
218 a reverse database, which were only identified by site, which were not quantified in every sample, or
219 which contained less than 2 unique peptides. Reporter ion intensity values were \log_2 transformed.
220 Each sample within a TMT set was then normalised to the average median intensity of all 12 samples
221 within that set. Moderated *t*-tests, with patient accounted for in the linear model, was performed
222 using Limma, where proteins with an adjusted $P < 0.05$ were considered as statistically significant.
223 Proteins with differential abundance (adjusted p-value < 0.05 and fold change > 1.5) were analysed
224 using the search tool for retrieval of interacting genes (STRING) database version 11 ([https://string-
226 db.org/](https://string-
225 db.org/)). The data was modified for presentation using Cytoscape version 3.7.2. Proteins were
227 grouped by functional categories based Uniprot annotation (<https://www.uniprot.org>). Active
228 interaction sources, including experiments and databases, and an interaction score > 0.7 were applied
229 to construct the protein-protein interaction networks. In the network, the nodes correspond to the
230 proteins identified and the edges represent the interactions. The node colour gradient depicts fold
231 change in protein expression in infected compared to mock samples. All analysis was performed using
232 R 3.6.2.
233